Z. Phys. B – Condensed Matter 89, 45–55 (1992)

Condensed Matter
Zeitschrift für Physik B

Dynamics of semi-infinite quantum spin chains at $T=\infty$

Joachim Stolze[1,*], **V.S. Viswanath**[2], **and Gerhard Müller**[2]

[1] Institut für Physik, Universität Dortmund, Postfach 500500, W-4600 Dortmund 50, Federal Republic of Germany
[2] Department of Physics, The University of Rhode Island, Kingston, RI 02881-0817, USA

Received March 30, 1992

Time-dependent spin autocorrelation functions and their spectral densities for the semi-infinite one-dimensional $s=\frac{1}{2}$ XY and XXZ models at $T=\infty$ are determined in part by rigorous calculations in the fermion representation and in part by the recursion method in the spin representation. Boundary effects yield valuable new insight into the different dynamical processes which govern the transport of spin fluctuations in the two models. The results obtained for the XXX model bear the unmistakable signature of spin diffusion in the form of a square-root infrared divergence in the spectral density.

1. Introduction

Exact results for time-dependent correlation functions of interacting quantum spin systems are scarce. With few exceptions [1], such results pertain to the one-dimensional $(1D)$ $s=\frac{1}{2}XY$ model, a system which can be transformed into a model of noninteracting fermions [2]. That model is the special case $\Delta=0$ of the more general $1D$ $s=\frac{1}{2}XYZ$ model. The XYZ Hamiltonian for a semi-infinite chain reads

$$H_{XYZ}=-J\sum_{l=0}^{\infty}\{(1+\gamma)S_l^xS_{l+1}^x+(1-\gamma)S_l^yS_{l+1}^y+\Delta S_l^zS_{l+1}^z\}. \tag{1.1}$$

The present study focuses on the boundary effects in the spin autocorrelation functions $\langle S_l^\mu(t)S_l^\mu\rangle$, $\mu=x,y,z$, at $T=\infty$.

What is the general behavior of spin autocorrelation functions at $T=\infty$ for systems with short-range interaction? That depends on the symmetry of the spin coupling. If the total spin component $S_T^\mu=\sum_l S_l^\mu$ is not conserved, the expectation is that the corresponding spin autocorrelation function is governed by a typical relaxation process, characterized by an exponential decay law,

$$\langle S_l^\mu(t)S_l^\mu\rangle\sim e^{-t/\tau}. \tag{1.2}$$

If S_T^μ is a conserved quantity, on the other hand, we expect the corresponding spin autocorrelation function to exhibit a diffusive long-time tail, characterized by an algebraic decay law:

$$\langle S_l^\mu(t)S_l^\mu\rangle\sim t^{-d/2}, \tag{1.3}$$

where d is the dimensionality of the system. It is a fact that none of the exactly known functions $\langle S_l^\mu(t)S_l^\mu\rangle$ is consistent with these expectations. There are good reasons for non-generic dynamics in the XY model, as will be discussed, but it has also remained unclear to what extent the $T=\infty$ dynamical properties of the more general XYZ model might be generic. (The $T=\infty$ spin correlation functions of Heisenberg chains were, for example, studied in [3] and [4] by means of short-time expansion techniques, mainly for spins far away from the chain ends. Further important progress in this direction was achieved recently by Böhm and Leschke [5]). As it turns out, the study of boundary effects is very useful for distinguishing and characterizing different dynamical processes for the transport of spin fluctuations.

We present new exact results for the XX and XY models, as determined in part by special methods and in part by a general method, and then we derive new results for the XXX and XXZ models by the same general method. That general method is the recursion method.

2. The XX model

Consider a semi-infinite chain of localized spins $\mathbf{S}_l$, $l=0$, 1, 2,... with nearest neighbors coupled as specified by the interaction Hamiltonian

* From April 1 to September 30, 1992 also at Institut für Physik, Universität Augsburg, W-8900 Augsburg, Federal Republic of Germany

$$H_{XX} = -J \sum_{l=0}^{\infty} \{S_l^x S_{l+1}^x + S_l^y S_{l+1}^y\}. \tag{2.1}$$

This is the XX model, the special case $\gamma = \Delta = 0$ of the more general XYZ model (1.1). For classical three-component spins, this is a model of nonlinear dynamics which is nonintegrable. There exists some evidence from simulation studies [6] that the spin autocorrelation functions exhibit generic behavior as outlined in Sect. 1, at least in the bulk limit ($l \to \infty$). That is manifestly not the case for quantum spins with $s = \frac{1}{2}$. The bulk spin autocorrelation functions $\langle S_\infty^\mu(t) S_\infty^\mu \rangle$ at $T = \infty$ and the associated spectral densities

$$\Phi_\infty^{\mu\mu}(\omega) = \int_{-\infty}^{+\infty} \mathrm{d}t \, \mathrm{e}^{\mathrm{i}\omega t} \langle S_\infty^\mu(t) S_\infty^\mu \rangle / \langle S_\infty^\mu S_\infty^\mu \rangle \tag{2.2}$$

have been determined exactly many years ago. The results for $\mu = z$,

$$\langle S_\infty^z(t) S_\infty^z \rangle = \tfrac{1}{4}[J_0(Jt)]^2 \tag{2.3a}$$

$$\Phi_\infty^{zz}(\omega) = \frac{2}{\pi J} K\left(\sqrt{1 - \frac{\omega^2}{4J^2}}\right) \Theta\left(1 - \frac{\omega^2}{4J^2}\right) \tag{2.3b}$$

were first derived by Niemeijer [7] and by Katsura et al. [8]. (J_0 denotes a Bessel function, $K(k)$ a complete elliptic integral of the first kind.) In the fermion representation of the XX model, the evaluation of these quantities is straightforward e.g. in terms of a two-particle Green's function for noninteracting lattice fermions. Note that the square of the Bessel function decays more rapidly, $\sim t^{-1}$, than (1.3) with $d = 1$, the prediction of spin diffusion phenomenology. Correspondingly, the complete elliptic integral in (2.3b) has only a logarithmic infrared divergence as opposed to the characteristic $\omega^{-\frac{1}{2}}$-divergence of $1D$ spin diffusion. The fluctuations of S_∞^z in this model are obviously not governed by a diffusive process despite the conservation law $S_T^z = \text{const}$. This is further demonstrated by the fact that fluctuations of S_q^z also decay algebraically, $\sim t^{-\frac{1}{2}}$ with oscillations, rather than exponentially, $\sim \exp(-Dq^2 t)$, as is expected for a diffusive process at least for small q.

The determination of the function $\langle S_\infty^x(t) S_\infty^x \rangle$ for that same model is far from straightforward despite its free-fermion nature. The exact result was, in fact, first conjectured by Sur et al. [9] on the basis of a moment analysis for finite chains. Rigorous derivations, based on the analysis of infinite Toeplitz determinants, were reported within one year by Brandt and Jacoby [10] and independently by Capel and Perk [11]. The result is a pure Gaussian as is then, of course, also its spectral density:

$$\langle S_\infty^x(t) S_\infty^x \rangle = \langle S_\infty^y(t) S_\infty^y \rangle = \tfrac{1}{4} \mathrm{e}^{-\frac{J^2 t^2}{4}} \tag{2.4a}$$

$$\Phi_\infty^{xx}(\omega) = \frac{2\sqrt{\pi}}{J} \mathrm{e}^{-\frac{\omega^2}{J^2}}. \tag{2.4b}$$

The Gaussian decay of (2.4a) is anomalous again. A normal relaxation process would be characterized by exponential decay. The non-generic processes that govern the transport of spin fluctuations in this model are further indicated by the fact that all pair correlations $\langle S_l^x(t) S_{l'}^x \rangle, l \neq l'$ are identically zero.

The free-particle nature of the excitation spectrum governing the correlation function $\langle S_\infty^z(t) S_\infty^z \rangle$ is readily recognizable by the bounded support of the spectral density $\Phi_\infty^{zz}(\omega)$ (2.3b). That same conclusion cannot be drawn from a mere inspection of the results (2.4a, b). Spectral densities with unbounded support are typical for the dynamics of interacting degrees of freedom. In order to detect the free-particle nature of the XX model in the xx-autocorrelation function, we must study boundary effects.

2.1. *Boundary effects in* $\langle S_l^z(t) S_l^z \rangle$

The zz-autocorrelation function was determined in closed form for all sites on the semi-infinite chain [12], [4]:

$$\langle S_l^z(t) S_l^z \rangle = \tfrac{1}{4}[J_0(Jt) - (-1)^{l+1} J_{2(l+1)}(Jt)]^2. \tag{2.5}$$

In the bulk limit $l \to \infty$, only the first term in the square bracket survives, and the result (2.3a) is recovered. The Fourier transforms of the Bessel functions $J_n(Jt)$ are nonzero only on the interval $[-J, J]$. The spectral density $\Phi_l^{zz}(\omega)$ associated with (2.5) is thus confined to the interval $[-2J, 2J]$. The singularity structure of $\Phi_l^{zz}(\omega)$ may be inferred from the long-time asymptotic expansion (LTAE) of the function (2.5), which has the following general structure:

$$\langle S_l^z(t) S_l^z \rangle \sim \sum_{n=0}^{\infty} a_n^l t^{-(2n+3)} + \left\{ \mathrm{e}^{2\mathrm{i}Jt} \sum_{n=0}^{\infty} b_n^l (\mathrm{i}t)^{-(n+3)} + \text{c.c.} \right\}. \tag{2.6}$$

The conclusion is that $\Phi_l^{zz}(\omega)$ has quadratic cusp singularities at the endpoints ($\omega = \pm 2J$) and exhibits quadratic behavior close to $\omega = 0$, independent of l. The bulk limit is subtle: the quadratic cusps at the endpoints become steeper and steeper and, for $l \to \infty$, transform into the discontinuities displayed by (2.3a). Likewise, the maximum at $\omega = 0$ grows higher and narrower and, for $l \to \infty$, turns into a logarithmic divergence.

These trends can be seen more clearly, when we note that the spectral density corresponding to the perfect square (2.5) may be written as the following self-convolution:

$$\Phi_l^{zz}(\omega) = \frac{8}{\pi J} \int_{\nu-1}^{1} \mathrm{d}\nu' \sqrt{1 - \nu'^2}\, U_l^2(\nu') \times \sqrt{1 - (\nu - \nu')^2}\, U_l^2(\nu - \nu') \quad (0 \leqq \omega/J \equiv \nu \leqq 2;\ \Phi_l^{zz}(-\omega) = \Phi_l^{zz}(\omega)). \tag{2.7}$$

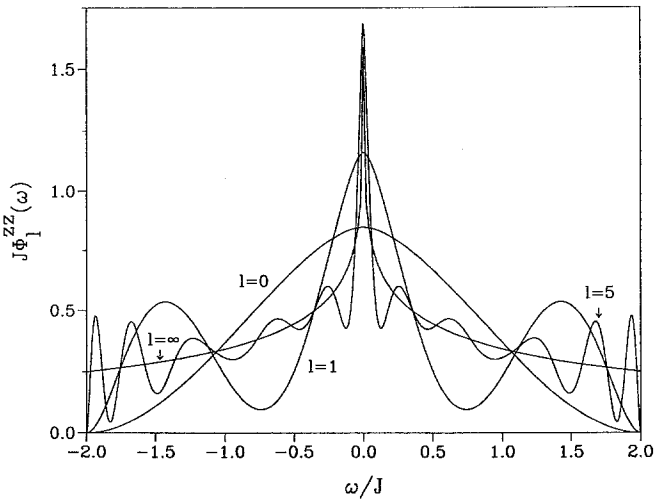

Fig. 1. Spectral density $\Phi_l^{zz}(\omega)$ for the $1D$ $s=\frac{1}{2}$ XX model at $T=\infty$ as determined by the Fourier transform of expression (2.5). The four curves represent the cases $l=0$ (boundary spin), $l=1, 5$, and $l=\infty$ (bulk spin)

Here U_l is a Tchebycheff polynomial of the second kind. The evaluation of the integral in (2.7) leads to cumbersome expressions involving elliptic integrals, but some useful insight can be deduced from it, nevertheless. For increasing l, the U_l have more and more oscillations. Convolution smears them out, but not entirely. For ω close to $2J$, (2.7) yields

$$\Phi_l^{zz}(\omega)=\frac{2}{J}(l+1)^4(2-\omega/J)^2 \quad (\omega \leqq 2J). \tag{2.8}$$

The l-dependent amplitude confirms the qualitative remarks made previously. The function $\Phi_l^{zz}(\omega)$ is singular at $\omega=0$ for any l. For example, expression (2.7) evaluated for the simplest case, $l=0$, yields

$$\Phi_0^{zz}(\omega)=\frac{128}{3\pi J}(1+\omega/2J) \times\left\{(1+\omega^2/4J^2)E\left(\frac{2J-\omega}{2J+\omega}\right) -\frac{\omega}{J}K\left(\frac{2J-\omega}{2J+\omega}\right)\right\}. \tag{2.9}$$

($E(k)$ and $K(k)$ are complete elliptic integrals.) For small ω the leading terms are

$$\Phi_0^{zz}(\omega)\sim a+\left(b+c\ln\left|\frac{\omega}{J}\right|\right)\omega^2. \tag{2.10}$$

The shape of the spectral density $\Phi_l^{zz}(\omega)$ for different values of l is shown in Fig. 1. In conclusion, the free-particle nature of the underlying dynamics is equally obvious in the spectral density $\Phi_l^{zz}(\omega)$ for sites near the boundary and in the bulk limit. That will no longer be the case when we investigate the spectral density $\Phi_l^{xx}(\omega)$ for the same model.

2.2. *Boundary effects in* $\langle S_l^x(t)S_l^x\rangle$

Here we discuss new explicit analytic results for the xx-autocorrelation functions $\langle S_l^x(t)S_l^x\rangle$ of the first few spins in a semi-infinite XX chain. A general determinantal expression for $\langle S_l^x(t)S_l^x\rangle$ is derived in Appendix A. That derivation uses the Jordan-Wigner transformation from spin-1/2 operators to Fermi operators and Wick's theorem, i.e. precisely the same techniques that were used to derive expression (2.5) for $\langle S_l^z(t)S_l^z\rangle$. The more complex structure of $\langle S_l^x(t)S_l^x\rangle$ as compared to that of $\langle S_l^z(t)S_l^z\rangle$ is best understood in the fermion representation: the spin operator S_l^z is simply mapped to a fermion number operator, but the operator S_l^x turns into a product of Fermi operators involving all of the sites between 0 and l. The function $\langle S_l^z(t)S_l^z\rangle$ may thus be evaluated as an expectation value of a product of four Fermi operators. The corresponding number of Fermi operators in $\langle S_l^x(t)S_l^x\rangle$ is $4l+2$. Wick's theorem must be applied for the evaluation of that function (see Appendix A for details about these well-known techniques and references to earlier work).

The general structure of the function $\langle S_l^x(t)S_l^x\rangle$ is a sum of products of integer-order Bessel functions $J_n(Jt)$ with $n=0, 1, \ldots, 2(l+1)$. Each term is the product of exactly $2l+1$ such functions. Explicit expressions for $l=0$, 1, 2, corresponding to the first three sites of a semi-infinite chain, are the following

$$\langle S_0^x(t)S_0^x\rangle=\tfrac{1}{4}(J_0+J_2), \tag{2.11}$$

$$\langle S_1^x(t)S_1^x\rangle =\tfrac{1}{4}\{(J_0+J_2) \times[(J_0+J_2)(J_0-J_4)+(J_1+J_3)^2]\}, \tag{2.12}$$

$$\begin{aligned}\langle S_2^x(t)S_2^x\rangle &=\tfrac{1}{4}[(J_0+J_2)(J_0-J_4)+(J_1+J_3)^2]\\ &\times\{(J_0+J_2)[(J_0-J_4)(J_0+J_6)+(J_1-J_5)^2]\\ &+(J_1+J_3)[(J_1+J_3)(J_0+J_6)\\ &+(J_1-J_5)(J_2+J_4)]\\ &+(J_2+J_4)[(J_1+J_3)(J_1-J_5)\\ &-(J_0-J_4)(J_2+J_4)]\}.\end{aligned} \tag{2.13}$$

Each Bessel function has the argument Jt. We have also evaluated explicit expressions for $l=3$, 4, but they are too lengthy to be reproduced here. The Fourier transform of any factor $(J_{i-j}\pm J_{i+j+2})$ is proportional to

$$U_i(\omega/J)\,U_j(\omega/J)\,\sqrt{1-\omega^2/J^2}\;\Theta(1-\omega^2/J^2).$$

Therefore, the spectral density $\Phi_l^{xx}(\omega)$ is a multiple convolution of $2l+1$ functions with compact support on the interval $[-J, J]$ and square-root singularities at the end points. The spectrum $\Phi_l^{xx}(\omega)$ thus is restricted to the interval $[-(2l+1)J, (2l+1)J]$, and we can expect non-divergent power-law singularities in $\Phi_l^{xx}(\omega)$ at frequen-

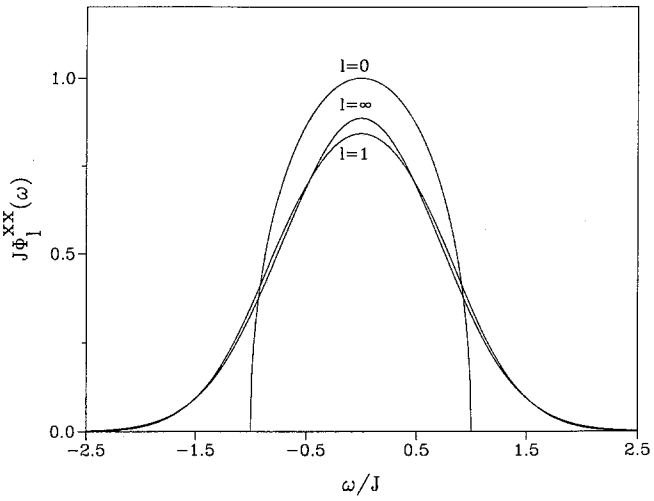

Fig. 2. Spectral density $\Phi_l^{xx}(\omega)$ for the $1D$ $s=\frac{1}{2}$ XX model at $T=\infty$. The three curves shown represent the cases $l=0, 1$ as determined by the Fourier transform of expressions (2.11) and (2.12), respectively, and the case $l=\infty$ given by the function (2.4b). The spectral densities for $l=2$ and $l=\infty$ coincide within line thickness

cies that are multiples of J. The convolution of $2l+1$ square-root singularities yields endpoint singularities of the form $\sim|\omega-(2l+1)J|^{3l+1/2}$. The actual endpoint singularity of $\Phi_l^{xx}(\omega)$, however, could be (and actually is) weaker due to cancellation effects. In order to obtain a more complete picture of the singularity structure of $\Phi_l^{xx}(\omega)$, we have analyzed the LTAE of $\langle S_l^x(t)S_l^x\rangle$. It has a considerably more complex structure than the one of $\langle S_l^z(t)S_l^z\rangle$:

$$\langle S_l^x(t)S_l^x\rangle \sim \sum_{m=0}^{l} C_m e^{i(2m+1)Jt}(it)^{-\gamma_m^{(l)}} \times \sum_{n=0}^{\infty} c_{mn}^{(l)}(it)^{-n}+\text{c.c.} \qquad (2.14)$$

with $\gamma_m^{(l)}=\frac{3}{2}+l(l+2)+m(m+1)$. The number of m-terms in (2.14) increases with l, the distance of the spin from the boundary. Each m-term in the LTAE (2.14) gives rise to a pair of (nondivergent) power-law singularities in $\Phi_l^{xx}(\omega)$ at frequencies $\omega_m=\pm(2m+1)J$. The associated singularity exponents, $\gamma_m^{(l)}-1$, increase monotonically with m and l; the exponent for the endpoint singularity is $2l^2+3l+1/2$, which indeed exceeds the value predicted by simple power-counting arguments. In the bulk limit, $l\to\infty$, the support of that spectral density is no longer bounded and all singularities fade away completely. The result is the Gaussian function (2.4b). In Fig. 2 we have plotted the exact results for $l=0$, 1, ∞. Convergence toward the bulk result (2.4b) is remarkably rapid.

The fact that $\Phi_l^{xx}(\omega)$ has compact support for finite l is the unmistakable signature of the free-particle nature of the underlying dynamics. That nature was not obviously recognizable in the bulk result $\Phi_\infty^{xx}(\omega)$ alone. It is interesting to compare these results with those previously found for the function $\langle S_\infty^x(t)S_\infty^x\rangle$ of the same model at $T=0$ [13], [14]. The LTAE consists of an infinite number of m-terms (see (2.9) of [14]) with leading exponents $\gamma_m^{(\infty)}=\frac{1}{2}[(m^2+1)/2]$, where $[x]$ denotes the integer part of x. The associated spectral density has unbounded support and an infinite sequence of singularities at frequencies $\omega_m=mJ$, $m=0$, 1, 2,.... The first two singularities ($m=0$, 1) are divergent. Boundary effects on the xx-correlation functions (both autocorrelations and pair correlations) of an XY chain at $T=0$ were studied by Pesch and Mikeska [15].

2.3. *Predictions of the recursion method*

To what extent would it have been possible to predict the exact results presented in Sects. 2.1 and 2.2 by the recursion method, i.e. by a general calculational technique that does not rely on the free-particle nature of the system? We investigate this question as a prelude to the study of the XXZ model, for which we shall employ the same general method. No special methods have been found for that model by which dynamic correlation functions can be determined exactly.

In the following we report a number of predictions for the spectral densities $\Phi_l^{zz}(\omega)$ and $\Phi_l^{xx}(\omega)$ of the XX model that can be extracted directly from the sequences of continued-fraction coefficients Δ_k produced by the recursion method. The formulation of the recursion method used here and outlined in Appendix B was developed by Lee [16] some ten years ago, but the analysis of the coefficients Δ_k presented in the following is of very recent origin [17], [18].

Consider first the spectral density $\Phi_l^{zz}(\omega)$. For $l=0$ the recursion method yields the Δ_k-sequence shown in Fig. 3 (main plot). Two quantitative properties of the function $\Phi_0^{zz}(\omega)$ can be extracted directly from these computational data: *(i)* The Δ_k tend to converge toward the value $\Delta_\infty=J^2$. The implication is that the spectral weight is confined to the frequency interval $|\omega|\leqq\omega_0=2\sqrt{\Delta_\infty}=2J$. *(ii)* The convergence toward the asymptotic value Δ_∞ is uniform in character. This indicates that $\Phi_0^{zz}(\omega)$ has only endpoint singularities, $\sim(\omega_0-\omega)^\beta$. The exponent β of that singularity determines the leading-order term of the large-k asymptotic expansion of the Δ_k-sequence [19]:

$$\Delta_k=\Delta_\infty\left[1+\frac{1-4\beta^2}{4k^2}+\ldots\right]. \qquad (2.15)$$

Uniform convergence from *below* means $\beta^2>\frac{1}{4}$. In the inset to Fig. 3, we have plotted the square-root of the quantity

$$\beta_k^2=\tfrac{1}{4}-k^2\left[\frac{\Delta_k}{\Delta_\infty}-1\right] \qquad (2.16)$$

versus $1/k$. The sequence $|\beta_k|$ tends to converge to the value $|\beta|=2$ rather convincingly. The recursion method thus would have correctly predicted the quadratic cusps of the exact result (2.9) (see Fig. 1).

For $1\leqq l<\infty$, the recursion method yields Δ_k-sequences that tend to converge toward the same value $\Delta_\infty=J^2$, but the approach is alternating in character for

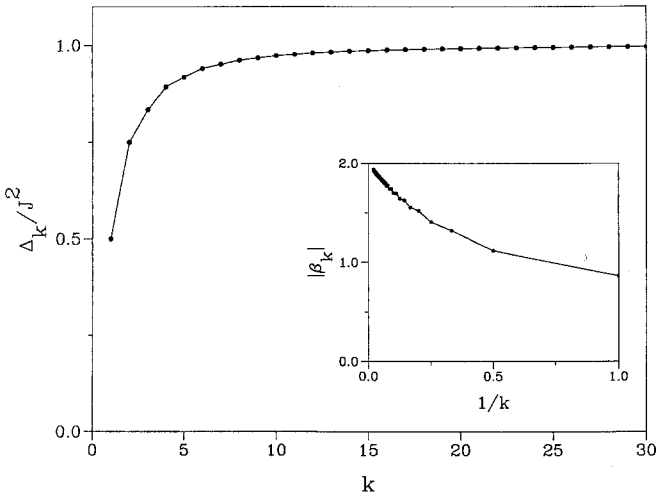

Fig. 3. Continued-fraction coefficients Δ_k (in units of J^2) vs. k, $k=1,\ldots,30$, for the spectral density $\Phi_0^{zz}(\omega)$ of the $1D$ $s=\frac{1}{2}$ XX model at $T=\infty$. The inset shows the sequence $|\beta_k|$ vs. $1/k$ for the same coefficients Δ_k (now up to $k=50$)

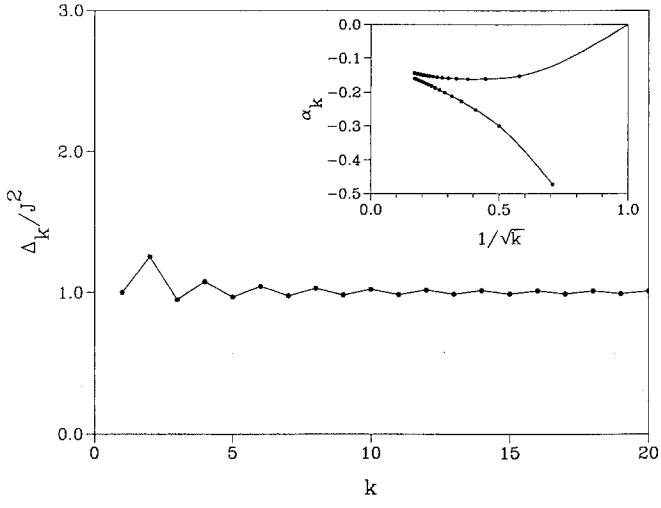

Fig. 4. Continued-fraction coefficients Δ_k (in units of J^2) vs. k, $k=1,\ldots,20$, for the spectral density $\Phi_\infty^{zz}(\omega)$ of the $1D$ $s=\frac{1}{2}$ XX model at $T=\infty$. The inset shows the sequence α_k vs. $1/\sqrt{k}$ for the same coefficients (now up to $k=35$)

k up to l (roughly) and then crosses over to uniform approach. The emerging new pattern indicates the buildup of an additional singularity at $\omega=0$ in the spectral density for $l\to\infty$. The Δ_k-sequence for the bulk case ($l=\infty$) is shown in Fig. 4. For spectral densities that have a power-law infrared singularity, $\sim|\omega|^\alpha$, the singularity exponent α is determined by the leading alternating term of the large-k asymptotic expansion of the Δ_k-sequence [18], [19]

$$\sqrt{\Delta_k}=\sqrt{\Delta_\infty}\left[1-(-1)^k\frac{\alpha}{2k}+\ldots\right]. \tag{2.17}$$

In the inset to Fig. 4 we have plotted the quantity

$$\alpha_k=(-1)^k 2k[1-\sqrt{\Delta_k/\Delta_\infty}] \tag{2.18}$$

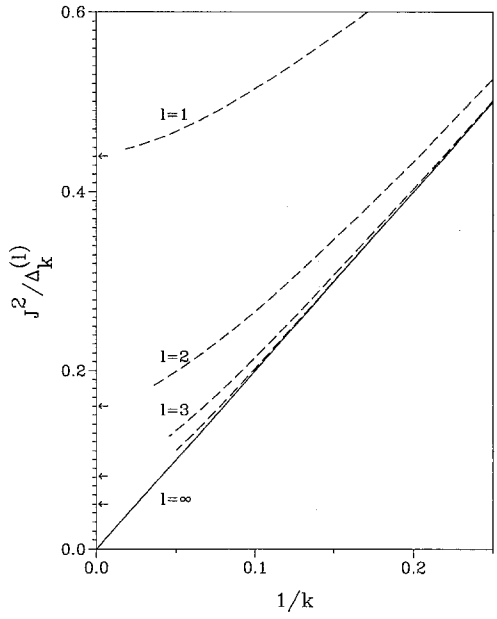

Fig. 5. Sequences $1/\Delta_k^{(l)}$ (in units of J^{-2}) plotted vs. $1/k$ for the spectral densities $\Phi_l^{xx}(\omega)$, $l=1, 2, 3, 4$, of the $1D$ $s=\frac{1}{2}$ XX model at $T=\infty$. The maximum value of k is 55, 28, 22, 20, for the four cases, respectively. The solid line represents the sequence for the bulk spin case ($l=\infty$). The arrows indicate the limiting values $1/\Delta_\infty^{(l)}$ for $l=1, 2, 3, 4$

versus $k^{-1/2}$. That sequence tends to converge to a negative value in the range between $\alpha=0$ and $\alpha=-0.1$, thus representing a weakly divergent singularity. This is consistent with the logarithmic divergence of the exact spectral density (2.3b).

Now we turn to the spectral density $\Phi_l^{xx}(\omega)$. For any finite l, the Δ_k-sequence tends to converge towards a finite value as $k\to\infty$. Our computational data are shown in Fig. 5. The dashed curves interpolate the values $1/\Delta_k^{(l)}$ plotted vs. $1/k$ for $l=1, 2, 3, 4$. The solid line represents the analytically known sequence, $\Delta_k^{(\infty)}=\frac{1}{2}J^2k$, for the bulk spin ($l=\infty$) [10, 20]. Not shown is the horizontal line which corresponds to the uniform sequence, $\Delta_k^{(0)}=\frac{1}{4}J^2$, for the boundary spin ($l=0$) [21]. All dashed curves start out superimposed on the solid curve up to $k=l$ and then level off gradually toward a finite value, $\Delta_\infty^{(l)}=\frac{1}{4}J^2(2l+1)^2$. This is consistent with the exactly known band edge, $\omega_0^{(l)}=(2l+1)J$, of the function $\Phi_l^{xx}(\omega)$ (see Sect. 2.2). The uniform convergence of the $\Delta_k^{(l)}$ toward their limiting values $\Delta_\infty^{(l)}$ is consistent with the fact that $\Phi_l^{xx}(\omega)$ does not have any infrared singularity.

The exponents $\beta^{(l)}$ of the endpoint singularities, $\sim(\omega_0^{(l)}-\omega)^{\beta^{(l)}}$, in the functions $\Phi_l^{xx}(\omega)$ can be determined directly from the $\Delta_k^{(l)}$ via (2.16), i.e. by means of extrapolation. For $l=0$, the square bracket in (2.16) vanishes identically, implying $|\beta^{(0)}|=\frac{1}{2}$ in agreement with the known square-root cusp of $\Phi_0^{xx}(\omega)$ (see Fig. 2). A simple extrapolation procedure applied to the sequences $\Delta_k^{(1)}$ and $\Delta_k^{(2)}$ reproduces the exact exponent values $\beta^{(1)}=\gamma_1^{(1)}-1=\frac{11}{2}$ and $\beta^{(2)}=\gamma_2^{(2)}-1=\frac{29}{2}$ to within one tenth of a percent and ond percent, respectively. More substantial deviations from the exact values are found for

$l=3$, where fewer coefficients $\Delta_k^{(l)}$ are availabe for analysis. There appears to be no practical means to extract any quantitative information on the interior singularities known to exist in the spectral densities $\Phi_l^{xx}(\omega)$ for $0<l<\infty$.

2.4. *The functions* $\langle S_0^x(t)\,S_0^x\rangle$ *and* $\langle S_0^y(t)\,S_0^y\rangle$ *for the XY model*

Consider a semi-infinite XY chain, specified by Hamiltonian (1.1) with $\Delta=0$ and $\gamma\neq 0$. This model can be mapped on to a free-fermion system with a gap at the Fermi surface. The gap disappears for the special case $\gamma=0$ (XX model). Dynamic spin correlation functions can be determined exactly, at least in principle. No such functions have ever been evaluated in closed form for $T=\infty$ to the best of our knowledge. (Pesch and Mikeska [15] obtained general determinantal expressions for $T=0$). Interestingly, the recursion method produces the exact results for the spectral densities $\Phi_0^{xx}(\omega)$ and $\Phi_0^{yy}(\omega)$ at $T=\infty$ with little calculational effort. The δ_k-sequences found for these two functions happen to exhibit a very simple pattern:

$$\Delta_{2k-1}^{xx}=\Delta_{2k}^{yy}=\tfrac{1}{4}J^2(1-\gamma)^2 \tag{2.19a}$$

$$\Delta_{2k-1}^{yy}=\Delta_{2k}^{xx}=\tfrac{1}{4}J^2(1+\gamma)^2. \tag{2.19b}$$

For the exact determination of the associated spectral densities, consider a sequence of continued-fraction coefficients that is periodic with period two: $\Delta_{2k-1}=\Delta_o, \Delta_{2k}=\Delta_e$. The continued-fraction representation of the relaxation function $c_0(z)$ specified by those coefficients can be terminated by the function itself at level two [22]:

$$c_0(z)=\cfrac{1}{z+\cfrac{\Delta_o}{z+\Delta_e c_0(z)}}. \tag{2.20}$$

(This had also been recognized by Sen [23], who used this information for a numerical analysis of the short-time behavior of the functions $\langle S_0^x(t)\,S_0^x\rangle$ and $\langle S_0^y(t)\,S_0^y\rangle$.) The solution of this quadratic equation yields, via (B.11), the following closed-form expression for the associated spectral density:

$$\begin{aligned}\Phi_0(\omega)=&\frac{1}{\Delta_e}\left[2(\Delta_o+\Delta_e)-\omega^2-\frac{(\Delta_o-\Delta_e)^2}{\omega^2}\right]^{-\frac{1}{2}}\\ &\times\Theta(|\omega|-\omega_{\min})\,\Theta(\omega_{\max}-|\omega|)\\ &+\frac{\pi}{\Delta_e}[\,|\Delta_o-\Delta_e|-(\Delta_o-\Delta_e)]\,\delta(\omega)\end{aligned} \tag{2.21}$$

with

$$\omega_{\min}=|\sqrt{\Delta_o}-\sqrt{\Delta_e}|,\ \omega_{\max}=\sqrt{\Delta_o}+\sqrt{\Delta_e}. \tag{2.22}$$

Applying this result to the sequences (2.19) for $\gamma>0$, we find that both spectral densities $\Phi_0^{xx}(\omega)$ and $\Phi_0^{yy}(\omega)$ have a continuum part confined to the frequency intervals $\omega_{\min}<|\omega|<\omega_{\max}$ and with square-root cusp singularities at each endpoint. The spectral density $\Phi_0^{xx}(\omega)$ has also a δ-function contribution at $\omega=0$.

The implication is that the boundary-spin autocorrelation function $\langle S_0^x(t)\,S_0^x\rangle$ decays algebraically to a nonzero constant asymptotically for $t\to\infty$. (This is indeed visible but not commented on in the numerical results presented in [23].) Such behavior is highly anomalous for a many-body system at $T=\infty$, attributable to the free-particle nature of the $s=\frac{1}{2}XY$ model. For $T=0$ Pesch and Mikeska [15] observed that $\langle S_l^x(t)\,S_m^x\rangle$ does not decay to zero as $t\to\infty$ for any l,m, because the system has long-range order at $T=0$. Returning to $T=\infty$ and setting $\gamma=0$ (XX model), we have $\Delta_o=\Delta_e=\Delta$; expression (2.21) reduces to

$$\Phi_0(\omega)=\frac{1}{\Delta}\sqrt{4\Delta-\omega^2}; \tag{2.23}$$

the gap and the δ-function have disappeared.

3. The XXZ model

The XXZ Hamiltonian

$$H_{XXZ}=-J\sum_{l=0}^{\infty}\{S_l^xS_{l+1}^x+S_l^yS_{l+1}^y+\Delta S_l^zS_{l+1}^z\} \tag{3.1}$$

is obtained by adding a coupling between the z-components of neighboring spins to the XX system (2.1). This amounts to introducing a density-density interaction in the fermion representation. Not surprisingly, the fermion interaction increases the complexity in the structure of dynamic correlation functions dramatically. That manifests itself perhaps most strikingly in the boundary-spin autocorrelation function $\langle S_0^x(t)\,S_0^x\rangle$ and the associated spectral density $\Phi_0^{xx}(\omega)$. A rigorous analysis is no longer within reach, and a perturbation calculation for weak fermion interaction, $|\Delta|\ll 1$, is highly impractical for this dynamical quantity. However, the application of the recursion method (in the spin representation) to that task is straightforward and requires only a modest amount of computational power.

We begin with the analysis of the case $\Delta=1$ (XXX model). The sequence $\Delta_k^{(0)}$ of continued-fraction coefficients produced by the recursion method for the boundary-spin spectral density $\Phi_0^{xx}(\omega)$ is plotted in the inset to Fig. 6. Notice the dramatic change from the sequence $\Delta_k^{(0)}=\frac{1}{4}J^2=\text{const}$, which characterizes the same spectral density for the XX model ($\Delta=0$, free fermions).

Δ_k-sequences as produced by the recursion method have been categorized quite generally according to their growth rate [3, 24]. The growth rate λ is defined as the power of k with which a given Δ_k-sequence grows on average:

$$\Delta_k\sim k^{\lambda}. \tag{3.2}$$

That quantity is known to determine the decay law of the associated spectral density at high frequencies [19], [25]:

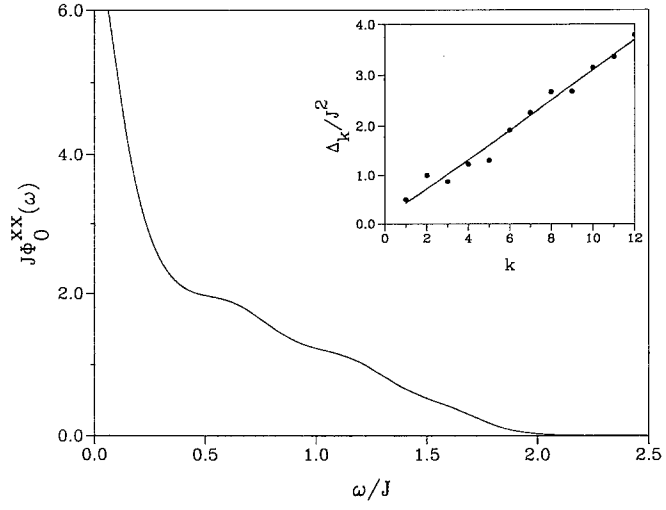

Fig. 6. Spectral density $\Phi_0^{xx}(\omega)$ (in units of J^{-1}) for the $1D$ $s=\frac{1}{2}$ XXX model ($\Delta=1$) at $T=\infty$. The result shown is derived from the continued-fraction representation of $c_0(\varepsilon-i\omega)$ (with $\varepsilon=0.001\,J$) terminated at level $n=12$ by means of a Gaussian terminator with parameter value $\omega_0=0.76\,J$. The Δ_k that have been used are shown (in units of J^2) in the inset together with the regression line $\frac{1}{2}\omega_0^2 k+c$, which determines the parameter value ω_0 and is used for the determination of the singularity exponent α

$$\Phi_0(\omega)\sim\exp(-\omega^{2/\lambda}). \tag{3.3}$$

In the case of the XXZ model, the sequence crosses over from $\lambda=0$ for $\Delta=0$ to $\lambda\simeq 1$ for $\Delta\neq 0$. The effect of the fermion interaction on the one-particle Green's function is a transformation of its spectral density from a function with bounded support to one with unbounded support and (roughly) Gaussian decay at high frequencies.

It must be mentioned at this point that the sequences $\Delta_k^{(l)}$ (plotted in Fig. 5) that characterize the spectral densities $\Phi_l^{xx}(\omega)$ for the noninteracting case ($\Delta=0$) also change from $\lambda=0$ for finite l to $\lambda=1$ in the bulk limit ($l=\infty$). In that case, however, the transformation of the spectral density from bounded to unbounded support is attributable to the nonlocality of the spin operator S_l^x in the fermion representation.

Switching from $\Delta=0$ to $\Delta=1$ also changes the rotatioal symmetry of H_{XXZ} in spin space in a way that has a drastic effect on the correlation function under investigation. Since the total spin component S_T^x is conserved for $\Delta=1$, we can expect that the spin autocorrelation function $\langle S_0^x(t)\,S_0^x\rangle$ is governed by a diffusive long-time tail of the form (1.3) with $d=1$. As a consequence of that property, the corresponding spectral density is expected to exhibit a strong infrared singularity, $\Phi_0^{xx}(\omega)\sim\omega^{-\frac{1}{2}}$.

Infrared singularities in spectral densities with unbounded support have their reflection in the Δ_k-sequences too. For a prototype case with $\lambda=1$ consider the model spectral density [18]

$$\Phi_0(\omega)=\frac{2\pi}{\omega_0\Gamma\left(\frac{\alpha}{2}-\frac{1}{2}\right)}\left|\frac{\omega}{\omega_0}\right|^{\alpha}\exp(-\omega^2/\omega_0^2) \tag{3.4}$$

and the associated Δ_k-sequence

$$\Delta_{2k-1}=\tfrac{1}{2}\omega_0^2(2k-1+\alpha),\qquad \Delta_{2k}=\tfrac{1}{2}\omega_0^2(2k). \tag{3.5}$$

For this prototype case, the singularity exponent α is determined by the displacement of the Δ_{2k-1} from the line $\Delta_{2k}=\omega_0^2 k$. Under more general circumstances, i.e. for a spectral density with a more complicated structure, the exponent α of its infrared singularity could be determined, for example, from the average distance in vertical displacement of the Δ_{2k} and the Δ_{2k-1} from the linear regression line that was derived for the entire sequence.

Looking at the graph $\Delta_k^{(0)}$ vs. k in Fig. 6 we can tell that the $\Delta_{2k}^{(0)}$ are displaced upwardly on average with respect to the $\Delta_{2k-1}^{(0)}$. This indicates that α is negative, i.e. the infrared singularity is divergent. The most we can hope to extract from the 12 known coefficients $\Delta_k^{(0)}$ is a reasonable estimate for the singularity exponent. Our result,

$$\alpha=-0.5\pm 0.4 \tag{3.6}$$

strongly suggests that $\Phi_0^{xx}(\omega)$ has a divergence at $\omega=0$, and the strength of the singularity is consistent with that predicted by spin diffusion phenomenology.

The 12 explicitly known continued-fraction coefficients $\Delta_k^{(0)}$ can also be used for the direct reconstruction of the spectral density $\Phi_0^{xx}(\omega)$ by means of a technique that was developed in [17]. The main idea at the basis of that technique is that the incomplete continued fraction (B.10) must be terminated by a termination function that is consistent with some general properties (growth rate, limiting value, etc.) of the explicitly known (finite) Δ_k-sequence.

For applications to Δ_k-sequences with roughly linear growth rate ($\lambda=1$), the Gaussian terminator is the least biased choice. In that case the reconstruction of the desired spectral density starts out from a Gaussian model spectral density according to a well defined procedure. A detailed description of that procedure can be found in [17], [18] for two applications to zero-temperature spin dynamics. In the present application, the coefficients $\Delta_k^{(0)}$ shown in the inset to Fig. 6 yield the reconstructed spectral density $\Phi_0^{xx}(\omega)$ shown in the main plot of that same figure. Its only distinctive feature is the characteristic spin-diffusive peak at $\omega=0$.

Our interpretion of the spectral density shown in Fig. 6 in terms of a simple $1D$ spin diffusion process will be more convincing if we can demonstrate that the sharp central peak disappears upon removal of the conservation law on which that process hinges: $S_T^x=\text{const}$. Therefore let us analyze the anisotropic case $\Delta=0.5$ of Hamiltonian (3.1), which violates that conservation law.

We have calculated the continued-fraction coefficients $\Delta_k^{(0)}$ for that case up to $k=11$ by means of the recursion method. It turns out that the growth rate determined for that (finite) sequence is significantly larger than $\lambda=1$, namely $\lambda=1.18\pm 0.04$. This modification calls for a generalization of both our methods *(i)* for estimating the singularity exponent α and *(ii)* for reconstructing the spectral density $\Phi_0^{xx}(\omega)$. Both tasks require a fair amount

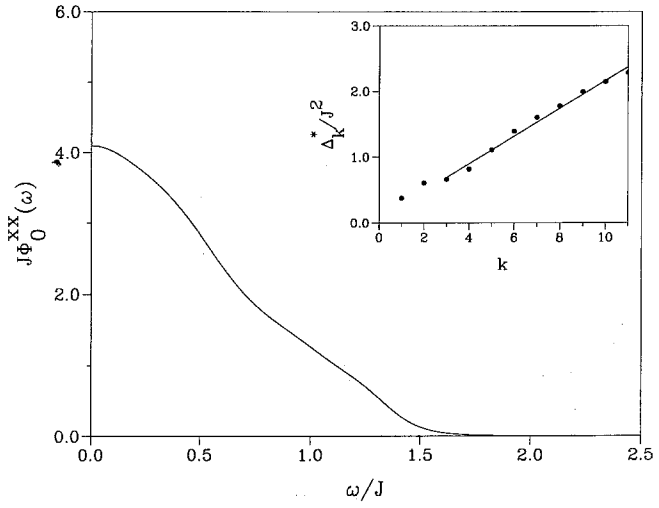

Fig. 7. Spectral density $\Phi_0^{xx}(\omega)$ (in units of J^{-1}) for the 1D $s=\frac{1}{2}$ XXZ model ($\Delta=0.5$) at $T=\infty$. The result shown is derived from the continued-fraction representation of $c_0(\varepsilon-i\omega)$ (with $\varepsilon=0.001\,J$) terminated at level $n=10$ by means of a Gaussian terminator with parameter value $\omega_0=0.65\,J$. The rescaled coefficients Δ_k^* that have been used are shown (in appropriately rescaled units) in the inset together with the regression line $\frac{1}{2}\omega_0^2 k+c$, which determines the parameter ω_0 and is used for the determination of the singularity exponent α

of developmental work, which is worthwhile to be invested. For this one application, however, we wish to take a shorter route.

For growth rates sufficiently close to $\lambda=1$, it can safely be argued that if one replaces the Δ_k-sequence by the sequence $\Delta_k^*=\Delta_k^{1/\lambda}$ and then proceeds with the analysis as in the previous application, the distortions resulting from unmatched growth rates are minimal. The rescaled sequence Δ_k^*vs. k up to $k=11$ is shown in the inset of Fig. 7. Notice that the alternating character of the deviations from the linear regression line has virtually disappeared. A quantitative analysis of the singularity exponent α from those deviations yields the following result:

$$\alpha=0.0\pm0.3\,. \tag{3.7}$$

Although this estimate has only limited predictive power, it is consistent with the disappearance of the spin-diffusive $\omega^{-\frac{1}{2}}$-divergence. That conclusion is confirmed by the spectral density $\Phi_0^{xx}(\omega)$ reconstructed from the first 11 coefficients $\Delta^*{}_k$ and a Gaussian terminator as outlined previously. That function is shown in the main plot of Fig. 7 and is to be compared with the result shown in Fig. 6. Note that the sharp central peak conspicuously present for $\Delta=1$ has completely disappeared in the anisotropic case, $\Delta=0.5$. This is precisely what is expected if the transport of spin fluctuations is governed by spin diffusion.

J.S. is grateful to Prof. Werner Weber for generous computer support, and to Dr. Andreas Giesekus for valuable help with the computer algebra. Support by the Deutsche Forschungsgemeinschaft through the Graduiertenkolleg Festkörperspektroskopie is gratefully acknowledged. The work done at URI was supported by the U.S. National Science Foundation, Grant DMR-90-07540. Access to supercomputers at the National Center for Supercomputing Applications, University of Illinois at Urbana-Champaign and at NASA-Ames Research Center is gratefully acknowledged. G.M. owes thanks to the University of Dortmund and to the University of Basel for their hospitality at the time this work was in progress. The research done in Basel was supported by the Swiss National Science Foundation.

Appendix A. Analytical results for $\langle S_l^x(t)\,S_l^x\rangle$

Here we derive analytical results for the xx-autocorrelation of an arbitrary spin l in the semi-infinite-spin-1/2 XX chain at infinite temperature. As already stated in [4], the calculation involves determinants of increasing size as l grows. We derive a general determinant expression from which the explicit results for $l=0,1,2$ quoted in Sect. 2.2 may be obtained. (The determinant structure of $\langle S_l^x(t)\,S_l^x\rangle$ was mentioned by Gonçalves and Cruz [12], but we are unaware of any explicit results for $0<l<\infty$.)

The spin ladder operators

$$S_l^{\pm}=(S_l^x\pm iS_l^y) \tag{A.1}$$

fulfill fermion-like anticommutator relations "on site", however, two operators acting on different sites commute. This cumbersome algebraic structure is simplified by the well-known Jordan-Wigner transformation [26]

$$S_l^+=(-1)^{\sum_{k=0}^{l-1}a_k^\dagger a_k}\,a_l^\dagger\,. \tag{A.2}$$

The a_l and $a_l^\dagger$ are fermion operators, $a_l^\dagger$ creates a particle at site l from the vacuum:

$$|l\rangle=a_l^\dagger|0\rangle\,. \tag{A.3}$$

In terms of fermion operators, the XX Hamiltonian (2.1) of an N-site chain ($l=0,\ldots,N-1$) reads

$$H_{XX}=-\frac{J}{2}\sum_{l=0}^{N-2}(a_l^\dagger a_{l+1}+a_{l+1}^\dagger a_l)\,. \tag{A.4}$$

The normalized one-particle eigenstates $|\nu\rangle$ of H_{XX} are given by

$$\langle l|\nu\rangle=\left(\frac{2}{N+1}\right)^{\frac{1}{2}}\sin\left(\frac{\nu\pi\,(l+1)}{N+1}\right)\quad(\nu=1,\ldots,N) \tag{A.5}$$

and the corresponding energy eigenvalues are

$$\varepsilon_\nu=-J\cos\left(\frac{\nu\pi}{N+1}\right). \tag{A.6}$$

Consequently, the Hamiltonian now reads

$$H_{XX}=\sum_{\nu=1}^{N}\varepsilon_\nu\,a_\nu^\dagger a_\nu \tag{A.7}$$

where the operator $a_\nu^\dagger$ creates a fermion in the state $|\nu\rangle$. Next we user the simple identity (valid for fermion op-

erators)

$$(-1)^{a_l^\dagger a_l} = 1 - 2a_l^\dagger a_l = (a_l^\dagger + a_l)(a_l^\dagger - a_l) =: A_l B_l \quad \text{(A.8)}$$

to rewrite the spin autocorrelation function as a correlation function involving the fermionic operators A_l and B_l defined by (A.8):

$$\langle S_l^x(t) S_l^x(0)\rangle = \tfrac{1}{4}\langle A_0(t) B_0(t) A_1(t) B_1(t) \ldots \times A_l(t) A_0 B_0 A_1 B_1 \ldots A_l\rangle . \quad \text{(A.9)}$$

This looks like a complicated representation of the sign generated by the Jordan-Wigner transformation (A.2) but it possesses an essential advantage: as A_l and B_l are linear combinations of Fermi operators, Wick's theorem may be applied to evaluate the expectation value. At first sight, the task looks cumbersome, because the right-hand side of (A.9) contains a product of $4l+2$ operators. However, if we write Wick's theorem in terms of Pfaffians [27], it is possible to keep track of the various terms:

$$\langle C_1 C_2 \ldots C_N\rangle = \begin{vmatrix} \langle C_1 C_2\rangle & \langle C_1 C_3\rangle & \ldots & \langle C_1 C_N\rangle \\ & \langle C_2 C_3\rangle & \ldots & \langle C_2 C_N\rangle \\ & & \ldots & \ldots \\ & & & \ldots \\ & & & \langle C_{N-1} C_N\rangle \end{vmatrix} = \pm (\det (C_{ij}))^{\frac{1}{2}} . \quad \text{(A.10)}$$

Here, $C_1, \ldots, C_N$ are linear combinations of fermion creation and annihilation operators, and the brackets denote equilibrium expectation values with respect to a bilinear fermion Hamiltonian. The triangular array in (A.10) is the usual way to write the Pfaffian, which is equal to the square root of the determinant of an antisymmetric matrix (C_{ij}) with an even number of rows and columns, defined by

$$C_{ij} = \langle C_i C_j\rangle \quad (1 \leqq i < j)$$
$$C_{ji} = -C_{ij} . \quad \text{(11)}$$

Like a determinant, a Pfaffian can be expanded with respect to the elements of any of its lines, where "line i" is the set of all elements carrying the index i, either as the first or second index. A minor of a Pfaffian is again a Pfaffian, generated by deleting two lines (i and j, say), and the adjoint of element (i, j) is the corresponding minor, with sign $(-1)^{i+j+1}$. For example:

$$\langle C_1 C_2 C_3 C_4\rangle = \begin{vmatrix} \langle C_1 C_2\rangle & \langle C_1 C_3\rangle & \langle C_1 C_4\rangle \\ & \langle C_2 C_3\rangle & \langle C_2 C_4\rangle \\ & & \langle C_3 C_4\rangle \end{vmatrix} = \langle C_1 C_2\rangle\langle C_3 C_4\rangle - \langle C_1 C_3\rangle\langle C_2 C_4\rangle + \langle C_1 C_4\rangle\langle C_2 C_3\rangle . \quad \text{(A.12)}$$

For the determination of the time-dependent correlation function (A.9) we thus have to evaluate the following Pfaffian:

$$4\langle S_l^x(t) S_l^x(0)\rangle = \begin{vmatrix} \langle A_0(t) B_0(t)\rangle & \langle A_0(t) A_1(t)\rangle & \ldots & \langle A_0(t) A_0\rangle & \langle A_0(t) B_0\rangle & \ldots & \langle A_0(t) A_l\rangle \\ & \langle B_0(t) A_1(t)\rangle & \ldots & \langle B_0(t) A_0\rangle & \langle B_0(t) B_0\rangle & \ldots & \langle B_0(t) A_l\rangle \\ & & \ldots & \ldots & \ldots & \ldots & \ldots \\ & & & \ldots & \ldots & \ldots & \ldots \\ & & & & \ldots & \ldots & \ldots \\ & & & & & \ldots & \ldots \\ & & & & & & \langle B_{l-1} A_l\rangle \end{vmatrix} \quad \text{(A.13)}$$

For the evaluation of the elements of this Pfaffian at $T = \infty$ we use

$$A_l(t) = \left(\frac{2}{N+1}\right)^{\frac{1}{2}} \sum_{\nu=1}^{N} \sin\frac{\nu\pi(l+1)}{N+1} \times (a_\nu^\dagger e^{i\varepsilon_\nu t} + a_\nu e^{-i\varepsilon_\nu t}), \quad \text{(A.14)}$$

and

$$\langle a_\nu^\dagger a_\mu\rangle = \langle a_\nu a_\mu^\dagger\rangle = \tfrac{1}{2}\delta_{\mu\nu} . \quad \text{(A.15)}$$

The result is

$$\langle A_l(t) A_m(t')\rangle = \frac{1}{N+1}\sum_{\nu=1}^{N}\left(\cos\frac{\nu\pi}{N+1}(l-m) - \cos\frac{\nu\pi}{N+1}(l+m+2)\right)\cos\varepsilon_\nu(t-t') . \quad \text{(A.16)}$$

For $N \to \infty$ the sum becomes an integral which is readily evaluated to yield

$$\langle A_l(t) A_m(t')\rangle = \begin{cases} 0 & \text{for } l-m \text{ odd} \\ (-1)^{\frac{l-m}{2}} f_{lm}(t-t') & \text{for } l-m \text{ even} . \end{cases} \quad \text{(A.17)}$$

Here we have introduced the shorthand notation

$$f_{lm}(t) := J_{l-m}(Jt) - (-1)^{(m+1)} J_{l+m+2}(Jt) , \quad \text{(A.18)}$$

and the J_n are Bessel functions. It is important to note that f_{lm} vanishes for $t = 0$, except for $l = m$. The following relations hold:

$$\langle A_l(t) A_m(t')\rangle = \langle A_m(t) A_l(t')\rangle = -\langle B_l(t) B_m(t')\rangle . \quad \text{(19)}$$

In an analogous manner we obtain

$$\langle A_l(t) B_m(t')\rangle = \begin{cases} i(-1)^{\frac{l-m-1}{2}} f_{lm}(t-t') & \text{for } l-m \text{ odd} \\ 0 & \text{for } l-m \text{ even} . \end{cases} \quad \text{(A.20)}$$

and

$$\langle A_l(t)\, B_m(t')\rangle = -\langle B_l(t)\, A_m(t')\rangle = \langle A_m(t)\, B_l(t')\rangle . \tag{A.21}$$

Hence, all elements of (A.13) with two equal time arguments vanish, which is a majority. All nonzero elements are located in the "upper right quadrant" of the Pfaffian. They form a $(2l+1)\times(2l+1)$ square matrix which may be conveniently written in terms of 2×2 blocks:

$$\begin{pmatrix} f_{00}\sigma^z & f_{01}\sigma^y & -f_{02}\sigma^z & -f_{03}\sigma^y & \cdots \\ f_{01}\sigma^y & f_{11}\sigma^z & f_{12}\sigma^y & -f_{13}\sigma^z & \cdots \\ -f_{02}\sigma^z & f_{12}\sigma^y & f_{22}\sigma^z & f_{23}\sigma^y & \cdots \\ -f_{03}\sigma^y & -f_{13}\sigma^z & f_{23}\sigma^y & f_{33}\sigma^z & \cdots \\ \vdots & \vdots & \vdots & \vdots & \ddots \end{pmatrix} \tag{A.22}$$

In this expression we have omitted the common time argument t from the functions f_{lm}; σ^y and σ^z are Pauli matrices. Considering the relation (A.10) between the Pfaffian and the determinant of an antisymmetric $(4l+2)\times(4l+2)$ matrix, it is easy to see that a Pfaffian of the type described above is (apart from the sign) equal to the determinant of the $(2l+1)\times(2l+1)$ matrix (A.22).

Appendix B. Formulation of the recursion method for quantum spin dynamics

For a given quantum spin Hamiltonian $H(\mathbf{S}_1,\ldots,\mathbf{S}_N)$, the time evolution of any dynamical variable $A(\mathbf{S}_1\ldots,\ldots,\mathbf{S}_N)$, here assumed to be a Hermitian operator, is determined by the Heisenberg equation of motion (with $\hbar\equiv 1$)

$$\frac{\mathrm{d}A}{\mathrm{d}t} = i[H,A] = iLA , \tag{B.1}$$

where $L=[H]$, is the quantum Liouville operator expressed as a commutator. That commutator is well defined in terms of the fundamental commutators of the spin algebra:

$$[S_l^\alpha, S_{l'}^\beta] = i\delta_{ll'}\sum_\gamma \varepsilon_{\alpha\beta\gamma} S_l^\gamma . \tag{B.2}$$

The recursion method for the calculation of the autocorrelation function $\langle A(t)\, A(0)\rangle$ is based on an orthogonal expansion of the associated dynamical variable:

$$A(t) = \sum_{k=0}^{\infty} C_k(t)\, f_k . \tag{B.3}$$

The orthogonal vectors f_k (Hermitian operators) are generated recursively via the Gram-Schmidt orthogonalization procedure with L as the generator of new directions:

$$f_{k+1} = iL f_k + \Delta_k f_{k-1} , \qquad k=1,2,\ldots \tag{B.4}$$

$$\Delta_k = (f_k, f_k)/(f_{k-1}, f_{k-1}) \tag{B.5}$$

with initial condition $f_0 = A$, $f_{-1}\equiv 0$. The scalar product in (B.5) is defined as the symmetrized canonical average,

$$(A,B) = \tfrac{1}{2}\langle AB+BA\rangle = \frac{1}{Z}\,\mathrm{Tr}[\mathrm{e}^{-\beta H}(AB+BA)] . \tag{B.6}$$

The sequence of non-negative numbers Δ_k thus determined contains all the information necessary for the reconstruction of the function $\langle A(t)\, A(0)\rangle$. Upon insertion of the orthogonal expansion (B.3) into the equation of motion (B.1) we obtain a set of linear differential equations for the functions $C_k(t)$:

$$\dot{C}_k(t) = C_{k-1}(t) - \Delta_{k+1} C_{k+1}(t) , \qquad k=0,1,2,\ldots . \tag{B.7}$$

with $C_{-1}(t)\equiv 0$, $C_k(0)=\delta_{k,0}$, and where

$$C_0(t) = \frac{(A(t), A(0))}{(A(0), A(0))} = \tfrac{1}{2}\frac{\langle A(t)\, A(0)\rangle + \langle A(0)\, A(t)\rangle}{\langle A(0)\, A(0)\rangle} \tag{B.8}$$

is the symmetrized and normalized autocorrelation function we wish to determine. It is the real part of $\langle A(t)\, A(0)\rangle/\langle A^2\rangle$; the imaginary part contains no additional information and can be determined from the relation

$$\langle A(-t)\, A(0) = \langle A(t-i\beta)\, A(0)\rangle = \langle A(t)\, A(0)\rangle^* .$$

Equations (B.7), converted by Laplace transform into a set of algebraic equations,

$$z c_k(z) - \delta_{k,o} = c_{k-1}(z) - \Delta_{k+1} c_{k+1}(z) , \qquad k=0,1,2,\ldots \tag{B.9}$$

with $c_{-1}(z)\equiv 0$, can be solved for the relaxation function in the continued-fraction representation:

$$c_0(z) \equiv \int_0^\infty \mathrm{d}t\, \mathrm{e}^{-zt} C_0(t) = \cfrac{1}{z + \cfrac{\Delta_1}{z + \cfrac{\Delta_2}{z+\cdots}}} . \tag{B.10}$$

The spectral density is obtained from (B.10) via the relation

$$\Phi_0(\omega) \equiv \int_{-\infty}^{+\infty} \mathrm{d}t\, \mathrm{e}^{\mathrm{i}\omega t} C_0(t) = 2 \lim_{\varepsilon\to 0} \mathrm{Re}\,[c_0(\varepsilon - \mathrm{i}\omega)] . \tag{B.11}$$

We have designed a FORTRAN program which calculates high-precision numerical values of the Δ_n for the spin autocorrelation functions $\langle S_l^\alpha(t)\, S_l^\alpha\rangle$ of the $1Ds = \frac{1}{2}XYZ$ model (1.1) at $T=\infty$. Owing to the property

$(S_l^\alpha)^2 = \frac{1}{4}$ of spin-$\frac{1}{2}$ operators, the vectors f_n produced by the orthogonalization scheme (B.4, B.5) have the following general structure (for $f_0 \equiv S_0^\alpha$):

$$f_n = \sum_{m=1}^{M(n)} a_m(n) \prod_{l=0}^{n} \prod_{\alpha=xyz} S_l^\alpha . \tag{B.12}$$

Since the S_l^α have zero trace, the evaluation of the norms is greatly simplified:

$$(f_n, f_n) = \sum_{m=1}^{M(n)} [a_m(n)]^2 . \tag{B.13}$$

For most applications of interest, only a limited number of continued-fraction coefficients Δ_k can be determined in practice. If the number of known coefficients Δ_k is not too small, valuable information on the structure of the associated spectral density can safely be predicted directly from that set of numbers. Examples are discussed in Sects. 2 and 3. That information can then be used for the reconstruction of the detailed shape of $\Phi_0(\omega)$ by a special method of terminating continued fractions, a method that was introduced in ([17], [18]).

References

1. Liu, J.-M., Müller, G.: Phys. Rev. A**42**, 5854 (1990); Phys. Rev. B**44**, 12020 (1991); Dekeyser, R., Lee, M.H.: Phys. Rev. B**43**, 8123, 8131 (1991); report exact results for spin systems with equivalent-neighbor interaction
2. Lieb, E., Schultz, T., Mattis, D.: Ann. Phys. (N.Y.) **16**, 407 (1961); Katsura, S.: Phys. Rev. **127**, 1508 (1962)
3. Roldan, J.M.R., McCoy, B.M., Perk, J.H.H.: Physica A**136**, 255 (1986)
4. Brandt, U., Stolze, J.: Z. Phys. B - Condensed Matter **64**, 327 (1986)
5. Böhm, M., Leschke, H.: J. Phys. A**25**, 1043 (1992)
6. Gerling, R., Landau, D.P.: Phys. Rev. B**42**, 8214 (1990)
7. Niemeijer, Th.: Physica **36**, 377 (1967)
8. Katsura, S., Horiguchi, T., Suzuki, M.: Physica **46**, 67 (1970)
9. Sur, A., Jasnow, D., Lowe, I.J.: Phys. Rev. B**12**, 3845 (1975)
10. Brandt, U., Jacoby, K.: Z. Phys. B - Condensed Matter **25**, 181 (1976)
11. Capel, H.W., Perk, J.H.H.: Physica A**87**, 211 (1977)
12. Conçalves, L.L., Cruz, H.B.: J. Magn. Magn. Mater. **15-18**, 1067 (1980)
13. McCoy, B.M., Perk, J.H.H., Shrock, R.E.: Nucl. Phys. B**220** [FS8], 35, 269 (1983)
14. Müller, G., Shrock, R.E.: Phys. Rev. B**29**, 288 (1984)
15. Pesch, W., Mikeska, H.J.: Z. Phys. B - Condensed Matter **30**, 177 (1978)
16. Lee, M.H.: Phys. Rev. B**26**, 2547 (1982)
17. Viswanath, V.S., Müller, G.: J. Appl. Phys. **67**, 5486 (1990)
18. Viswanath, V.S., Müller, G.: J. Appl. Phys. **70**, 6178 (1991)
19. Magnus, A.: In: The recursion method and its applications. Pettifor, D.G., Weaire, D.L. (eds.), p. 22. Berlin, Heidelberg, New York: Springer 1985
20. Florencio, J., Lee, M.H.: Phys. Rev. B**35**, 1835 (1987)
21. Sen, S., Mahanti, S.D., Cai, Z.-X.: Phys. Rev. B**43**, 10990 (1991)
22. More generally, if the Δ_k-sequence has periodicity n, then the continued-fraction representation of the coresponding relaxation function can be terminated by that function itself at level n
23. Sen, S.: Phys. Rev. B**44**, 7444 (1991)
24. See first paper of [1]
25. Lubinsky, D.S.: Acta Appl. Math. **10**, 237 (1987)
26. For an extensive discussion of the Jordan-Wigner transformation between spin-1/2 operators and fermion operators as applied to the solution of the one-dimensional XY model see [2]. The first paper also contains some historical remarks on the origin of this transformation
27. The most important properties of Pfaffians and some comments on their relation to Wick's theorem may be found, e.g. In: Caianiello, E.R.: Combinatorics and renormalization in quantum field theory. Reading, Mass.: W. A. Benjamin 1973; and In: Green, H.S., Hurst, C.A.: Order-disorder phenomena. London: Wiley-Interscience 1964